

Lumbar sympathectomy accelerates sacrococcygeal wound healing in rats.

Zhifang Zheng^{1,2}, Yishu Liu^{2,3}, Xuan Min², Jianbing Tang², Biao Cheng^{1,2,3,4,5*}

¹The Graduate School of Southern Medical University, Guangzhou, PR China

²Department of Plastic Surgery, Guangzhou General Hospital of Guangzhou Military Command, Guangzhou, PR China

³The Graduate School of Third Military Medical University, Chongqing, PR China

⁴Center of Wound Treatment, Guangzhou General Hospital of Guangzhou Military Command, Guangzhou, PR China

⁵The Key Laboratory of Trauma Treatment and Tissue Repair of Tropical Area, PLA, Guangzhou, PR China

Abstract

Pressure Ulcers (PUs) severely impair patient quality of life and account for a high percentage of annual healthcare costs. Lumbar sympathectomy has previously been used for the treatment of chronic leg ulcers. It is still unclear, however, whether lumbar sympathectomy accelerates wound healing in sacrococcygeal skin, a high-risk area for PUs in mostly bedridden patients. Thirty-six Sprague Dawley rats were randomly assigned to the lumbar sympathectomised group, the sham-operated group, and the blank control group. Two wounds were generated in the sacrococcygeal skin of each rat 2 w after modelling. The expression of dopamine β -hydroxylase (D β H) and Norepinephrine (NE) in sacrococcygeal skin were detected by immunohistochemistry and western blotting. The wounds were photographed and measured with Image-Pro Plus v 6.0 software. Then, the wounds were cut and observed by haematoxylin and eosin staining for re-epithelialization and Masson's Trichrome staining for collagen fibres on d 3, 7, and 21 post-wounding. D β H and NE expression in sacrococcygeal skin were reduced 2 w after sympathectomy. Lumbar sympathectomy accelerated sacrococcygeal wound contraction ($p < 0.05$). There were no statistical differences among groups in the scores of reepithelialisation. The integrated optical densities of stained collagen were increased after sympathectomy in sacrococcygeal wounds ($p \leq 0.001$). In conclusion, lumbar sympathectomy accelerates sacrococcygeal wound healing in rats. Lumbar sympathectomy may be beneficial for the healing of PUs in the sacrococcygeal region.

Keywords: Lumbar sympathectomy, Local sympathetic denervation, Pressure ulcers, Wound contraction.

Accepted on May 12, 2017

Introduction

Pressure Ulcers (PUs) and leg ulcers are common in clinical practice. They constitute serious problems, severely impair patient quality of life, and account for a high percentage of annual healthcare costs [1,2]. Acute leg ulcers tend to occur after serious injury (trauma) or surgery. Chronic leg ulcers may be divided into venous leg ulcers, Diabetic Foot Ulcers (DFUs), PUs, and arterial ulcers [3]. PUs in the sacrococcygeal region may be due to limited mobility from brain or spinal cord injuries or fractures [4].

The relationship between Norepinephrine (NE) and skin wound healing is still controversial. NE recruits innate immune cells and expedites wound closure in mice [5]. NE has been shown to promote neurotisation in connective tissue regenerates of skin wounds in white rats [6]. Grabovoi suggested that NE decreases the inflammatory reaction, the fibroblast content of the regenerate, and the degree of

cytoplasmic basophilia in white rats [7]. Furthermore, NE has been shown to inhibit the growth of fibroblasts taken from neonatal mice in an *in vitro* assay [8].

The sympathetic nervous system plays an important role in hard-to-heal wounds [9]. Thoracic sympathectomy is useful for digital ischemia and ulcers [10,11]. Lumbar sympathectomy improves the wound healing of diabetic feet [12], chronic venous leg ulcers [13], and critical limb ischemia [14-17]. NE is significantly associated with the development of pressure ulcers [18]. The sacrococcygeal skin is a high-risk area for PUs in mostly bedridden patients. However, it is still unclear whether lumbar sympathectomy accelerates skin wound healing in this region. This study aimed to explore the effects of lumbar sympathectomy on wound healing in the sacrococcygeal skin of rats.

Materials and Methods

Animals

Thirty-six male Sprague Dawley rats weighing 250-300 g were purchased from the animal centre of Southern Medical University, Guangzhou, China. Rats were acclimatised for 1 week prior to the surgical protocols. The animals were maintained at $23 \pm 1^\circ\text{C}$ with a 12 h light/dark cycle and free access to standard laboratory food and water. The ambient temperature in all animal experiments was kept at 25°C . The experiments were conducted according to institutional guidelines and were approved by the Animal Care Committee of Guangzhou General Hospital of Guangzhou Command.

Animal model

Thirty-six Sprague Dawley rats were randomly assigned to three groups: the sympathectomised group, the sham-operated group, and the blank control group. The sympathectomised group underwent lumbar sympathetic trunk (L2-4) resection with a surgical microscope (Leica M300, Germany). First, the posterior peritoneal attachments were freed, and the intestine, spleen, liver, and stomach were retracted to the right. A blunt dissection was then carried out to peel the peritoneal covering off of the posterior abdominal wall and to explore the gutter between the quadratus lumborum muscles overlying the vertebral column as previously described [19]. The lumbar sympathetic trunks L2-4 were pale and located anterior to the spine, medial to the genitofemoral nerves (Figure S1). The sham-operated group received an operation, but the lumbar sympathetic trunks were not removed. The blank control group underwent anaesthesia but no surgery. Intraoperative temperature changes in the hind plantar skin were recorded using a NeXus-10 MKII thermometer (Stens Biofeedback-Stens Corporation, San Rafael, CA, USA) in the sympathectomised group. The skin temperature of the left foot increased intraoperatively by 0.8°C , 30 min after lumbar sympathectomy (Figures S2 and S3).

In vivo wounding procedure and monitoring

Two weeks after modelling, the rats were anesthetized using 0.6% pentobarbital sodium (40 mg/kg) and two round, full-thickness dermal wounds (1.5 cm diameter, at a distance of 1.0 cm) were made on both sides of the sacrococcygeal skin in each rat using skin punches. The skin specimens in the sacrococcygeal region were sent for immunoenzyme staining and western blotting. After the wounding procedure, the animals were kept in separate cages. The wounds were photographed using a digital camera on d 3, 5, 7, 10, 14, and 21 post-wounding. The wound sizes were measured with Image-Pro Plus v 6.0 software and calculated against the original area (on d 0), which was designated as 100%. The wounds, including 0.5 mm wound edge tissues, were cut under anaesthesia for analyses in 4 rats (8 wounds) from each group on d 3, 7, and 21 post-wounding.

Haematoxylin and eosin staining

The harvested wounds were fixed in 10% neutral formalin, dehydrated in a graded series of ethanol, and then embedded in paraffin for routine haematoxylin and eosin (H and E) staining. As part of the histological evaluation, all slides were examined by a pathologist without knowledge of the previous treatment. Histological scoring of epidermal and dermal regeneration in this study was performed according to a previously described method [20].

Masson's trichrome staining

The wound specimens (scars) were fixed with formalin and embedded in paraffin according to routine laboratory techniques. Serial 5 μm thick sections were obtained and stained with Masson's Trichrome to detect collagen fibres. Deparaffinised sections were incubated with haematoxylin for 10 min, 0.5% hydrochloric acid alcohol for 3 s, and 0.6% ammonia for 30 s. After being washed with tap water for 1 min, sections were stained with Ponceau liquid for 1 hour and then washed for 1 min with tap water. After 5 min in phosphomolybdic acid solution, sections were stained for 5 min in water-soluble aniline blue and then incubated for 1 min with 1% acetic acid. After routine alcohol and xylene-based dehydration, the sections were fixed in 10% neutral buffered formalin for light microscopy. A pathologist who was blinded to the research design checked all the sections and described the pathological changes. In addition, Image-Pro Plus 6.0 was used to scan and sum the integrated optical density of the stained collagen as previously described [21].

The pathological deparaffinised sections of sacrococcygeal skin were washed three times in Phosphate Buffer Solution (PBS) for 5 min, and then blocked with 5% serum for 30 min. The slides were subsequently incubated at 4°C overnight with primary antibodies against NE (1:1000 dilution; Lifespan, Cambridge, UK) and dopamine β -hydroxylase (D β H; 1:800 dilution; Abcam, Cambridge, UK). After rinsing three times with PBS, the slides were incubated with secondary antibodies at 37°C for 30 min. The secondary antibodies were horseradish peroxidase-labelled antibodies, further developed with 3, 3'-diaminobenzidine tetrahydrochloride solution.

Western blotting

Sacrococcygeal skin tissue lysate was homogenized in a radioimmunoprecipitation assay buffer (50 mM Tris HCl pH 8, 150 mM NaCl, 1% NP-40, 0.5% sodium deoxycholate, 0.1% SDS, 2 mM EDTA, protease inhibitor cocktail, phosphatase inhibitor cocktail, and 1 mM DTT). The protein concentration was determined using the BSA method and the skin lysates were denatured at 95°C for 5 min in sodium dodecyl sulfate polyacrylamide gel electrophoresis (SDS-PAGE) loading buffer. Then, 40 μg of total protein was resolved in 12% SDS-PAGE and transferred to polyvinylidene fluoride membranes. The membranes were blocked with 5% fat-free dry milk in Tris-buffered saline containing 0.1% (v/v) Tween 20 (TBS-T) for 1 h at room temperature. After blocking, membranes were

incubated with primary antibodies against NE (1:1500 dilution) and DβH (1:3000 dilution) overnight at 4°C. The membranes were then washed and incubated for 1 h at room temperature with anti-rabbit antibody (1:20,000 dilution). The membranes were exposed to an enhanced chemifluorescence reagent followed by scanning using VersaDoc Imaging System (Bio-Rad Laboratories, Portugal). For normalisation, the membranes were reprobred with an anti-GAPDH antibody (1:10,000 dilution). The generated signals were analysed using Image-Quant TL software.

Statistical analysis

Data are expressed as mean ± Standard Deviation (SD). Statistical comparisons were performed using ANOVA (t-test). All statistical computations were performed using SPSS software, version 21.0 (IBM Corp., Armonk, NY, USA). Differences with a value of P<0.05 were considered statistically significant.

Results

Confirmation of local sympathetic denervation of sacrococcygeal skin

NE and DβH were located primarily in areas with arteriovenous anastomoses, arrector pilorum muscles, and arterioles; whereas, few adrenergic fibres were found around sweat glands (Figures 1 and 2). The expressions of NE (P<0.001) and DβH (P<0.001) were reduced 2 w after sympathectomy (Figure 3).

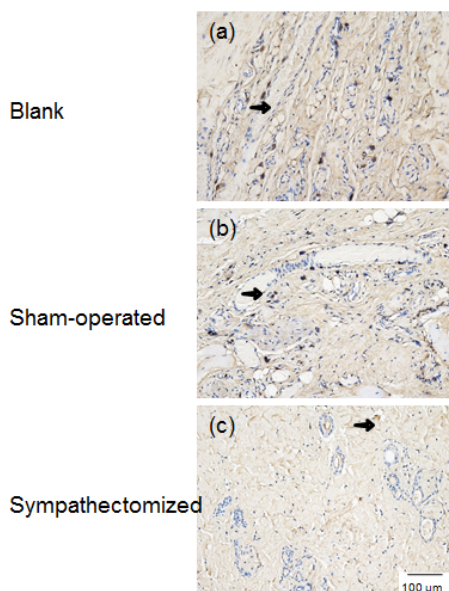


Figure 1. NE expression in the sacrococcygeal skin of rats 2 w after modelling. The bar corresponds to 100 μm. Arrows show positive staining.

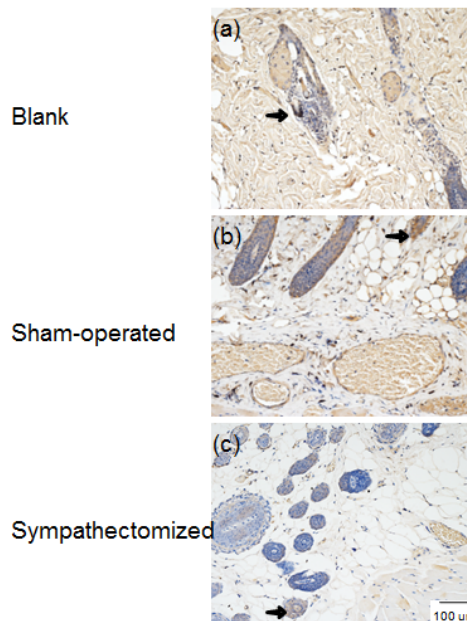


Figure 2. DβH expression in the sacrococcygeal skin of rats 2 w after modelling. The bar corresponds to 100 μm. Arrows show positive staining.

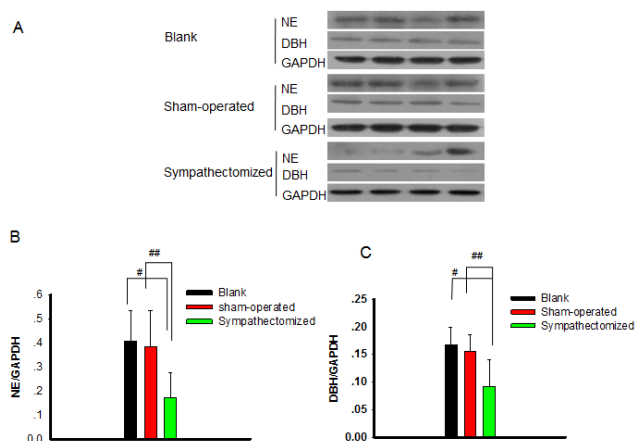


Figure 3. NE and DβH expression in the sacrococcygeal skin of rats 2 w after modelling. GAPDH was used as an internal control for clarity. Values shown represent mean ± standard deviation; n=12 specimens in each group. #p<0.001 for the sympathectomised group compared with the blank control group; ##p<0.001 for the sympathectomised group compared with the sham-operated group.

In vivo wound healing observations

From d 3 post-wounding, scabs caused by blood clots and fibrous tissue were observed. The wound areas in the blank control group were larger than those in the sympathectomised group on d 10 (p=0.019; Figures 4A and 4B). The wound areas in the sham-operated group were larger than those in the sympathectomised group on d 5 (p=0.018), d 10 (p=0.040), and d 14 (p=0.046; Figures 4A and 4B).

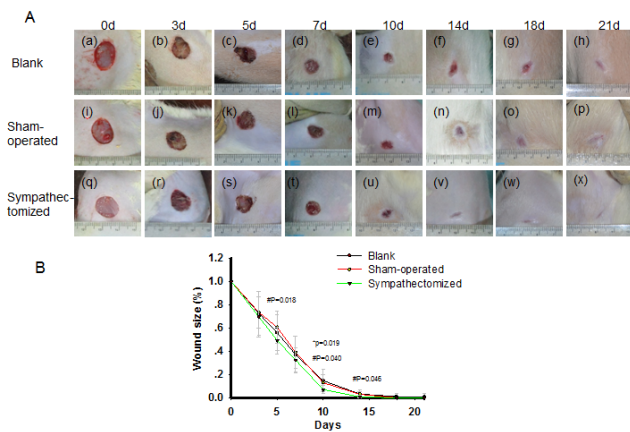


Figure 4. Wound size in the sympathectomized group, the sham-operated group, and the blank control group after full-thickness wounding in rats. (A) Shows the specific size of sacrococcygeal wounds at different time-points. (B) Indicates statistical differences in wound size. * $p < 0.05$ for the sympathectomized group compared with the blank control group; # $p < 0.05$ for the sympathectomized group compared with the sham-operated group.

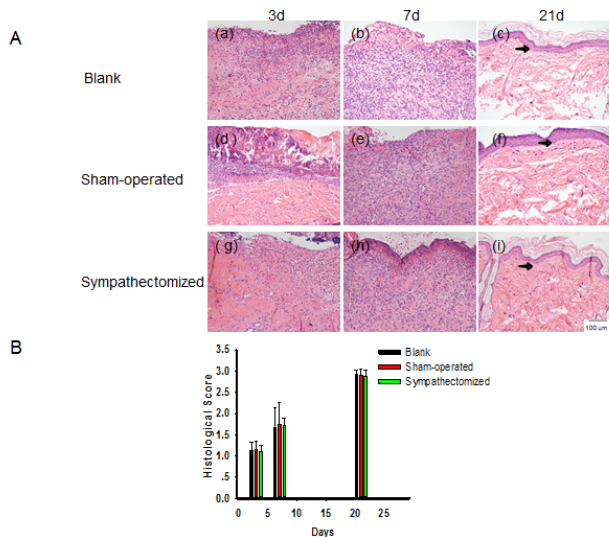


Figure 5. (A) Shows histological analyses of sacrococcygeal skin stained with H & E at different time-points after full-thickness wounding. The bar corresponds to 100 μ m. Arrows indicate the stratum basale. (B) Indicates the histological scores of the epidermal and dermal regeneration in sacrococcygeal wounds.

Haematoxylin and eosin staining

There were many inflammatory cells in the wounds during the early stages of healing. The number of collagen fibres increased throughout the period of wound healing. The wound surfaces were gradually covered by epidermal cells. There were no statistical differences among the groups in reepithelialisation scores (Figures 5A and 5B).

Masson's trichrome staining

The collagen fibres present in the skin wounds and wound edges increased throughout the period of wound healing

(Figure 6A). The integrated optical densities of stained collagen in the sympathectomized group were greater than those in the blank control group on d 7 ($p = 0.001$) and d 21 ($p < 0.001$; Figure 6B). Likewise, the integrated optical densities of stained collagen were greater in the sympathectomized group compared with the sham-operated group on d 7 ($p = 0.001$) and d 21 ($p < 0.001$; Figure 6B).

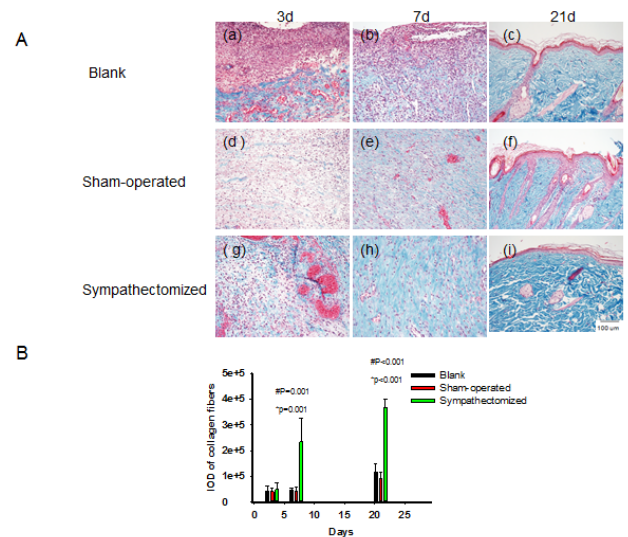


Figure 6. (A) Shows histological analyses of sacrococcygeal skin stained with Masson's Trichrome staining at different time-points after full-thickness wounding. The bar corresponds to 100 μ m. (B) Indicates the integrated optical densities in sacrococcygeal wounds; $n = 4$ specimens for each group at each time-point. * $p \leq 0.001$ for the sympathectomized group compared with the blank control group; # $p \leq 0.001$ for the sympathectomized group compared with the sham-operated group.

Discussion

In this experiment, all the rats survived after lumbar sympathectomy. The accuracy of lumbar sympathectomy was confirmed by intraoperative monitoring of skin temperatures (Figures S2 and S3). To avoid the potentially confounding effect of an operation-related stress response, the wounds in the sacrococcygeal skin were made 2 w after modelling.

NE and D β H are common sympathetic markers. D β H is one of the key enzymes in the synthesis of NE [22]. A major portion of the hind leg [23,24] and the femoral arteries [25] are innervated by L2 through L4 of the sympathetic chain. If the L2–4 sympathetic trunks are removed bilaterally, sympathetic nerve functions decline in the lower limbs [26]. Previous studies showed that tyrosine hydroxylase immunoreactive fibres were reduced in the rat superficial pineal gland on d 7, 14, 21, and 42 post-removal of the superior cervical ganglia [27,28]. Lindpaintner et al. [29] proved that bilateral stellate ganglionectomy led to profound decreases in cardiac NE and D β H 10 and 20 d after surgery in male guinea pigs. In our experiment, NE and D β H expression were reduced in the sacrococcygeal skin 2 w after lumbar sympathectomy in rats (Figures 1-3), indicating local sympathetic denervation.

PUs usually show delayed wound contraction. Lumbar sympathectomy is used to treat diabetic feet [12], chronic venous leg ulcers [13], and critical limb ischemia [14-17]. We first reported that lumbar sympathectomy could accelerate wound healing in sacrococcygeal skin (Figure 4). Lumbar sympathectomy did not change the re-epithelialisation rate, but it increased collagen fibre deposition to promote wound healing in sacrococcygeal skin (Figures 5 and 6). NE is significantly associated with the development of PUs [18]. Accelerated wound healing in the sacrococcygeal region may be associated with decreased NE after sympathectomy (Figures 1 and 3).

In conclusion, lumbar sympathectomy accelerates sacrococcygeal wound healing by increasing collagen fibre deposition. Lumbar sympathectomy may be useful for patients with wounds in the sacrococcygeal region.

Acknowledgements

This work was supported by the Guangzhou City Science and Technology Project (201508020253), the Guangzhou Province Science and Technology Project (2014B020212010), the National Natural Science Foundation of China (81171812, 81272105 and 81671924), and the National Basic Science and Development Program (2012CB518105).

References

1. Situm M, Kolic M, Redzepi G, Antolic S. Chronic wounds as a public health problem. *Acta Med Croatica* 2014; 68: 5-7.
2. Mooij MC, Huisman LC. Chronic leg ulcer: does a patient always get a correct diagnosis and adequate treatment? *Phlebology* 2016; 31: 68-73.
3. Kirsner RS, Vivas AC. Lower-extremity ulcers: diagnosis and management. *Br J Dermatol* 2015; 173: 379-390.
4. Bielecki M, Skowronski R, Skowronski J. Sacral pressure sores and their treatment. *Chir Narzadow Ruchu Ortop Pol* 2006; 71: 51-56.
5. Gosain A, Jones SB, Shankar R, Gamelli RL, DiPietro LA. Norepinephrine modulates the inflammatory and proliferative phases of wound healing. *J Trauma* 2006; 60: 736-744.
6. Grabovoi AN. Morphologic and histochemical changes of skin nervous apparatus in wound healing following local action of noradrenaline and acetylcholine. *Morfologija* 1999; 115: 68-72.
7. Grabovoi AN. Content of fibroblasts, macrophages, granulocytes and lymphocytes in the connective tissue regenerate of the skin in wound healing as affected by noradrenaline, acetylcholine, propranolol and atropine. *Morfologija* 1999; 116: 41-45.
8. Saito T, Tazawa K, Yokoyama Y, Saito M. Surgical stress inhibits the growth of fibroblasts through the elevation of plasma catecholamine and cortisol concentrations. *Surg Today* 1997; 27: 627-631.
9. Pan L, Tang J, Liu H, Cheng B. Sympathetic nerves: How do they affect angiogenesis, particularly during wound healing of soft tissues? *Clin Hemorheol Microcirc* 2016; 62: 181-191.
10. Han KR, Kim C, Park EJ. Successful treatment of digital ulcers in a scleroderma patient with continuous bilateral thoracic sympathetic block. *Pain Physician* 2008; 11: 91-96.
11. Coveliers HM, Hoexum F, Nederhoed JH, Wisselink W, Rauwerda JA. Thoracic sympathectomy for digital ischemia: a summary of evidence. *J Vasc Surg* 2011; 54: 273-277.
12. Shor NA, Chumak Iu F, Reuka VP, Zhukov OA. Revascularization of the lower limbs for ischemic diabetic foot with pyonecrotic tissue lesions. *Angiol Sosud Khir* 2004; 10: 85-89.
13. Patman RD. Sympathectomy in the treatment of chronic venous leg ulcers. *Arch Surg* 1982; 117: 1561-1565.
14. Hatangdi VS, Boas RA. Lumbar sympathectomy: a single needle technique. *Br J Anaesth* 1985; 57: 285-289.
15. van Dielen FM, Kurvers HA, Dammers R, oude Egbrink MG, Slaaf DW, Tordoir JH, Kitslaar PJ. Effects of surgical sympathectomy on skin blood flow in a rat model of chronic limb ischemia. *World J Surg* 1998; 22: 807-811.
16. Tomlinson L. Case study to illustrate a multidisciplinary approach to a case of critical limb ischaemia and the role of chemical lumbar sympathectomy. *J Tissue Viability* 2000; 10: 140-143.
17. Rivers SP, Veith FJ, Ascer E, Gupta SK. Successful conservative therapy of severe limb-threatening ischemia: the value of nonsympathectomy. *Surgery* 1986; 99: 759-762.
18. Cox J, Roche S. Vasopressors and development of pressure ulcers in adult critical care patients. *Am J Crit Care* 2015; 24: 501-510.
19. Hweidi SA, Lee S, Wolf P. Effect of sympathectomy on microvascular anastomosis in the rat. *Microsurgery* 1985; 6: 92-96.
20. Altavilla D, Saitta A, Cucinotta D, Galeano M, Deodato B, Colonna M, Torre V, Russo G, Sardella A, Urna G. Inhibition of lipid peroxidation restores impaired vascular endothelial growth factor expression and stimulates wound healing and angiogenesis in the genetically diabetic mouse. *Diabetes* 2001; 50: 667-674.
21. Sun X, Kim YH, Phan TN, Yang BS. Topical application of ALK5 inhibitor A-83-01 reduces burn wound contraction in rats by suppressing myofibroblast population. *Biosci Biotechnol Biochem* 2014; 78: 1805-1812.
22. Mione MC, Sancesario G, D'Angelo V, Bernardi G. Increase of dopamine beta-hydroxylase immunoreactivity in non-noradrenergic nerves of rat cerebral arteries following long-term sympathectomy. *Neurosci Lett* 1991; 123: 167-171.
23. Dellon AL, Hoke A, Williams EH, Williams CG, Zhang Z, Rosson GD. The sympathetic innervation of the human foot. *Plast Reconstr Surg* 2012; 129: 905-909.

24. Catre MG, Salo PT. Quantitative analysis of the sympathetic innervation of the rat knee joint. *J Anat* 1999; 194: 233-239.
25. Peterson DF, Norvell JE. Sympathetic postganglionic pathways to the hind-limb of the rat: a fluorescent histochemical study. *J Auton Nerv Syst* 1985; 13: 171-174.
26. Flotte CT. Evaluation of lumbar sympathectomy. *Am J Cardiol* 1959; 4: 644-648.
27. Hernandez G, Bello AR, Lopez-Coviella I, Abreu P, Fajardo N, Reiter RJ, Hernandez A, Alonso R. Tyrosine hydroxylase activity in peripherally denervated rat pineal gland. *Neurosci Lett* 1994; 177: 131-134.
28. Zhang ET, Mikkelsen JD, Moller M. Tyrosine hydroxylase- and neuropeptide Y-immunoreactive nerve fibers in the pineal complex of untreated rats and rats following removal of the superior cervical ganglia. *Cell Tissue Res* 1991; 265: 63-71.
29. Lindpaintner K, Lund DD, Schmid PG. Role of myocardial hypertrophy in trophic stimulation of indices of sympathetic cardiac innervation. *J Cardiovasc Pharmacol* 1987; 10: 211-220.

***Correspondence to**

Biao Cheng

Department of Plastic Surgery

Guangzhou General Hospital of Guangzhou Military Command

PR China